

# Production of $^{92}\text{Y}$ via the $^{92}\text{Zr}(n,p)$ reaction using the $\text{C}(d,n)$ accelerator neutron source

Tadahiro Kin<sup>1,a</sup>, Yukimasa Sanzen<sup>1</sup>, Masaki Kamida<sup>1</sup>, Yukinobu Watanabe<sup>1</sup>, and Masatoshi Itoh<sup>2</sup>

<sup>1</sup> Department of Advanced Energy Engineering Science, Kyushu University, 6-1 Kasuga-koen, Kasuga, Fukuoka 816-8580, Japan

<sup>2</sup> Tohoku University, Cyclotron and Radioisotope Center, 6-3Aoba, Aramaki, Aoba-ku, Sendai, Miyagi 980-8578, Japan

**Abstract.** We have proposed a new method of producing medical radioisotope  $^{92}\text{Y}$  as a candidate of alternatives of  $^{111}\text{In}$  bioscan prior to  $^{90}\text{Y}$  ibritumomab tiuxetan treatment. The  $^{92}\text{Y}$  isotope is produced via the  $^{92}\text{Zr}(n,p)$  reaction using accelerator neutrons generated by the interaction of deuteron beams with carbon. A feasibility experiment was performed at Cyclotron and Radioisotope Center, Tohoku University. A carbon thick target was irradiated by 20-MeV deuterons to produce accelerator neutrons. The thick target neutron yield (TTNY) was measured by using the multiple foils activation method. The foils were made of Al, Fe, Co, Ni, Zn, Zr, Nb, and Au. The production amount of  $^{92}\text{Y}$  and induced impurities were estimated by simulation with the measured TTNY and the JENDL-4.0 nuclear data.

## 1. Background

Medical radioisotopes are widely used for diagnosis and therapeutic treatments. In particular, radioimmunotherapy (RIT) has played an increasingly important role over recent years in cancer therapy.  $^{90}\text{Y}$ -ibritumomab tiuxetan was the first RIT agent approved by the US Food and Drug Administration (USFDA), followed by more than 40 other countries [1–3]. Until November 2011, the assessment of biodistribution by means of  $^{111}\text{In}$ -ibritumomab tiuxetan before administration of  $^{90}\text{Y}$ -ibritumomab tiuxetan (called “bioscan”) was required in United States, Japan and Switzerland. The FDA removed the bioscan and the first reason was “analysis of data in 253 patients showed that the In-111 imaging dose and bioscan was not a reliable predictor of altered Y-90 Zevalin (the trade name of ibritumomab tiuxetan) bio-distribution” [4]. If ibritumomab tiuxetan is labelled with an yttrium isotope that emits positron or suitable gamma rays, such a procedure would constitute a reliable monitor by adoption of PET or gamma-ray imaging. As first demonstrated by Herzog et al. [5], the positron emitting  $^{86}\text{Y}$  was mixed with  $^{90}\text{Y}$  and PET studies were performed to determine the distribution of activity. However since PET is not commonly available, we propose to use a gamma emitting isotope of Y.

Yttrium-90m (682 keV,  $T_{1/2}=3.2\text{h}$ ),  $^{91\text{m}}\text{Y}$  (556 keV,  $T_{1/2}=50\text{m}$ ), and  $^{92}\text{Y}$  (934 keV,  $T_{1/2}=3.5\text{h}$ ) are candidates of the gamma-ray emitter. Both  $^{90\text{m}}\text{Y}$  and  $^{91\text{m}}\text{Y}$  decay from metastable states to unstable ground states and remain as undesirable source of  $\beta^-$  emissions in human body for the long terms (64 h and 59 d for  $^{90}\text{Y}$  and  $^{91}\text{Y}$ ). On the other hand,  $^{92}\text{Y}$  decays to stable isotope  $^{92}\text{Zr}$  and there is no risk of additional exposure caused by the

daughter nuclide. Therefore,  $^{92}\text{Y}$  is a promising candidate as an alternative for  $^{111}\text{In}$  bioscan prior to  $^{90}\text{Y}$  ibritumomab tiuxetan treatment.

## 2. Production method

The accelerator-based neutron method shows promise for the production of various medical radioisotopes [6]. In the method proposed,  $^{92}\text{Y}$  would be produced via the  $^{92}\text{Zr}(n,p)$  reaction based on an accelerator neutron source from  $\text{C}(d,n)$ . Since there is no suitable method to produce  $^{92}\text{Y}$ , we propose a new method based on the accelerator neutron method. Figure 1 shows the neutron excitation function of  $^{92}\text{Zr}$  stored in JENDL-4.0 [7]. For  $^{92}\text{Y}$  production reaction, the cross sections were consistent with experimental values by Majah et al. [8], Raics et al. [9], and Semkova et al. [10]. The threshold energy for the production cross section is approximately 5–7 MeV, and from that point on the value increases with neutron energy to reach a maximum around 17 MeV.

Among all by-products, the nuclides that cannot be separated by chemical processes should be taken into account to estimate the radioactive and isotopic purities of the  $^{92}\text{Y}$  product. Within the lower energy region, radioactive nuclides  $^{93}\text{Zr}$  and  $^{89}\text{Sr}$  are produced, but they can be readily removed by chemical processing of the irradiated target. As a stable isotope product, only  $^{89}\text{Y}$  should be considered as carrier. However, since the production cross section is lower by an order of magnitude to that of  $^{92}\text{Y}$ , the impact is negligible. In contrast, comparable amount of  $^{91}\text{Y}$  is produced via the  $(n,np)$  and  $(n,d)$  reaction in higher energy region. Because of the radioactivity, it affects not only isotopic but also radioactive purities. Therefore, the production amount should be kept in low level.

<sup>a</sup> e-mail: kin@aees.kyushu-u.ac.jp

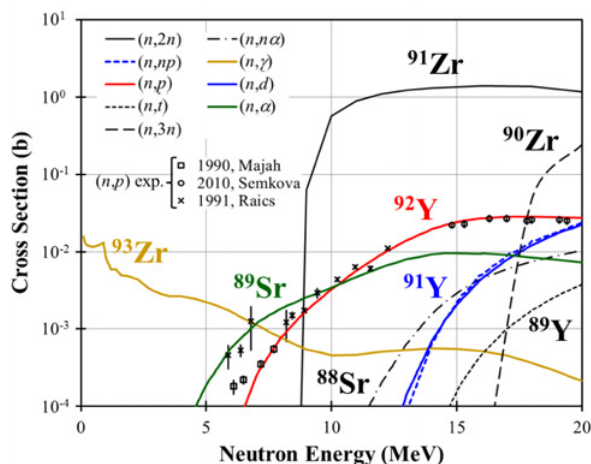


**Figure 1.** Excitation functions of neutron-induced reactions on  $^{92}\text{Zr}$ . The red, green, and blue lines show the production reaction of  $^{92}\text{Y}$ ,  $^{89}\text{Sr}$ , and  $^{91}\text{Y}$ , respectively.

As discussed above, the requirement of the neutron energy distribution to produce  $^{92}\text{Y}$  is summarized as follows;

- 1) High intensity is required near the energy that corresponds to the maximum cross section of  $^{92}\text{Zr}(n,p)$  reaction to produce sufficient amount of  $^{92}\text{Y}$ .
- 2) High-energy component of the neutron beam over 15 MeV should be avoided in order to suppress  $^{91}\text{Y}$ .

The  $C(d,n)$  reaction has been selected to generate neutrons, because the energy spectrum has a broad peak around half the incident deuteron energy as a consequence of elastic and non-elastic break-up reactions [11]. In other words, the energy distribution can be adjusted by selection of incident deuteron energy. Suitable energy range to produce the above-mentioned distribution is expected to be between 20 and 30 MeV.

In this paper, we consider neutron production from 20-MeV deuterons on thick carbon target as feasibility study. The aim of our paper is estimation of the  $^{92}\text{Y}$  production yields, the radioactive and isotopic impurities. They are able to estimate by multiplying the thick target neutron yield (TTNY) of the  $C(d,n)$  reaction by the production cross sections. However, only a few experimental data of the TTNYs of the  $C(d,n)$  reaction are available at incident energies between 20 and 30 MeV. Therefore, the TTNY needs to be measured prior to the estimations.

### 3. Experiment

The multiple foils activation method was adopted to measure the TTNY. A measurement of the TTNY of the  $C(d,n)$  reaction at 20 MeV was carried out at Cyclotron and Radioisotope Center (CYRIC), Tohoku University. Deuterons were accelerated to 20 MeV by the model 930 cyclotron, and were guided to and bombarded a 2-mm thick carbon target at a current of  $2 \mu\text{A}$  for 19 hours. The accelerator neutrons were transported to the metal foils made of Zn, Co, Nb, Zr, Mo, Au, Al, Ni, and Fe (for detail, see Table 1) placed at 0 degree to the deuteron beam.

After 30-minutes cooling, the gamma rays from the activated foils were measured by two HPGe detectors.

**Table 1.** The elements and the weight of the irradiation foils.

Element of Foil	Weight (g)
Al	0.173
Fe	0.391
Co	2.501
Ni	2.155
Zn	3.426
Zr	1.860
Mo	1.292

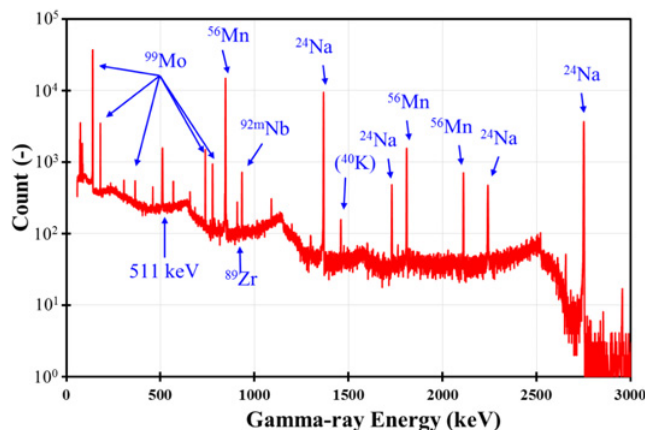


**Figure 2.** The gamma-ray spectrum of the activated Al, Mo, and Fe foils.

As  $^{56}\text{Mn}$  is produced via the  $^{56}\text{Fe}(n,p)$  and  $^{59}\text{Co}(n,\alpha)$  reactions, the foils were separated into a few groups to measure the two reaction rates individually. Gamma rays from  $^{152}\text{Eu}$ ,  $^{137}\text{Cs}$  and  $^{133}\text{Ba}$  standard sources were also measured by the Ge detectors for energy calibration and correction of peak detection efficiency.

### 4. Analysis

As an example, a gamma-ray spectrum of the group of activated Al, Mo, and Fe foils is shown in Fig. 2.

The nine nuclear reactions listed in Table 2 were considered in the multiple foils activation method. Yields of the product at the end of irradiation (EOI) were derived from the measured gamma-ray spectra, and the result is given in Table 2.

To derive the TTNY from these yields, unfolding method was adopted. We used the GRAVEL code [12], which uses a slight modification of the SAND-II algorithm for the unfolding process. Response functions were created from the excitation functions stored in JENDL-4.0 [7]. An initial TTNY was calculated with the DEURACS [11] and PHITS [13] codes as shown in Fig. 3 (for detailed explanations of the two codes, see Refs. [11, 13]).

### 5. Results and discussion

#### 5.1. Thick target neutron yield

The results of unfolding with different initial TTNY values are shown in Fig. 4. Although there is no large discrepancy between the two results, we use the TTNY unfolded by using DEURACS-TTNY in the following. This is because DEURACS calculations reproduce other experimental TTNYs reasonably well over a wide range

**Table 2.** The yields of the products induced via the nine reactions at the end of irradiation (EOI).

Reaction	No. of Atoms (-) at EOI
$^{27}\text{Al}(n,\alpha)^{24}\text{Na}$	$5.30(02) \times 10^7$
$^{56}\text{Fe}(n,p)^{56}\text{Mn}$	$1.28(01) \times 10^7$
$^{59}\text{Co}(n,\alpha)^{56}\text{Mn}$	$1.90(01) \times 10^7$
$^{59}\text{Co}(n,p)^{59}\text{Fe}$	$2.68(01) \times 10^8$
$^{58}\text{Ni}(n,2n)^{57}\text{Ni}$	$1.24(01) \times 10^7$
$^{64}\text{Zn}(n,p)^{64}\text{Cu}$	$6.91(10) \times 10^8$
$^{67}\text{Zn}(n,p)^{67}\text{Cu}$	$7.59(08) \times 10^6$
$^{96}\text{Zr}(n,2n)^{95}\text{Zr}$	$7.00(07) \times 10^7$
$^{96}\text{Mo}(n,p)^{96}\text{Nb}$	$1.63(02) \times 10^6$

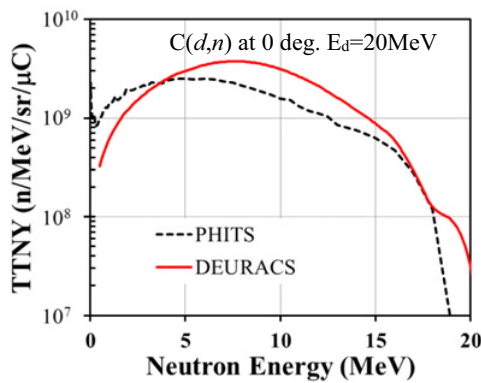


**Figure 3.** Initial approximation of the TTNy for  $C(d,n)$  reaction at 0 degree by 20-MeV deuterons as calculated by DEURACS and PHITS codes.

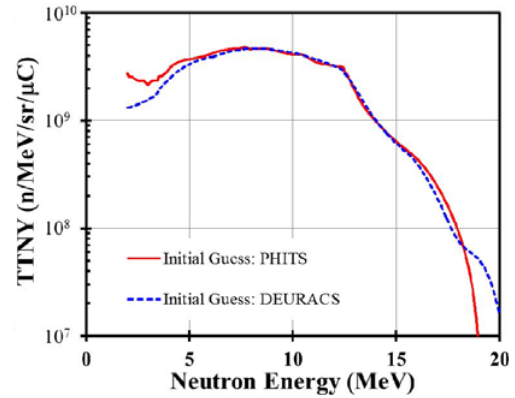
of emission energy at incident deuteron energies near 20 MeV, as shown in Ref. [11].

Figure 5 shows the energy-integrated value of the present TTNy together with those at 12-, 14-, 16-, and 18-MeV deuteron energies as measured by Weaver et al. [14]. The broken line in the figure is a linear fit of the values of Weaver et al. The extrapolated value at 20 MeV is  $4.04 \times 10^{10}$  n/sr/μC and it is in good agreement with the present value of  $4.33 \times 10^{10}$  n/sr/μC. Note that the values of Weaver et al. were obtained at 3.5 degrees to the direction of the incident deuteron beam, and are considered to be about 7% smaller than the value at 0 degree.

The production yields of the nine reactions listed in Table 2 are calculated by folding the present TTNy with the cross sections stored in JENDL-4.0. The ratio of the calculated yields to the experimental ones (C/E) are shown in Fig. 6, and demonstrate that the reproducibility of the production yields is sufficiently good.

## 5.2. Production yield and isotopic purity

Production yields of  $^{92}\text{Y}$  and by-products are calculated by multiplying the present TTNy by the cross sections stored in JENDL-4.0. In the estimation, the  $^{nat}\text{Zr}$  target of 20 g is placed at 0 degrees to the deuteron beam and 50 mm from the  $C(d,n)$  neutron source. The beam current is assumed to be 2 mA that is the same as in the GRAND project [6]. An irradiation time of 7.5 hours produce 75% of the saturation yield. Both the time variation of the induced



**Figure 4.** TTNy obtained by the unfolding process.

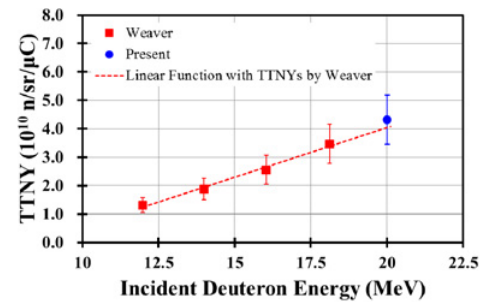


**Figure 5.** Energy-integrated values of present and Weaver TTNys as a function of incident deuteron energy.

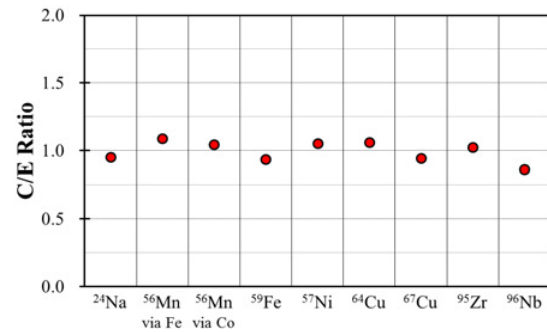


**Figure 6.** C/E ratio of the production yields of nine reactions.

radioactivity and the ratio of the number of carriers from the EOI are shown in Fig. 7(a) and (b), respectively. Note that the branching ratios of the isomer and ground state populations are calculated by the CCONE code [15, 16].

The summed activity of  $^{90m}\text{Y}$  and  $^{90g}\text{Y}$  is more than 5 times higher than that of  $^{92}\text{Y}$ . As the activity of  $^{89}\text{Zr}$  is very high, this radioactive impurity needs to be separated by means of a suitable chemical process. Stable carrier  $^{89}\text{Y}$  is also produced at 34 times the rate of  $^{92}\text{Y}$ , and may be a main cause of low labelling efficiency. Potential isotopic impurities within  $^{92}\text{Y}$  needs to be addressed with care – problematic by-products are produced via the  $^{90}\text{Zr}(n,np)^{89}\text{Y}$ ,  $^{91}\text{Zr}(n,np)^{90}\text{Y}$ ,  $^{91}\text{Zr}(n,d)^{90}\text{Y}$ ,  $^{91}\text{Zr}(n,p)^{91}\text{Y}$ ,  $^{92}\text{Zr}(n,np)^{91}\text{Y}$ ,  $^{92}\text{Zr}(n,d)^{91}\text{Y}$ , and  $^{90}\text{Zr}(n,2n)^{89}\text{Zr}$  reactions. Almost all of the reactions can be suppressed by using enriched  $^{92}\text{Zr}$  apart from the last two reactions. As shown in Fig. 1, the production cross section of  $^{91}\text{Y}$  by neutron-induced reactions on  $^{92}\text{Zr}$  is small. Thus, we concluded that isotopically enriched  $^{92}\text{Zr}$  should be used for  $^{92}\text{Y}$  production.

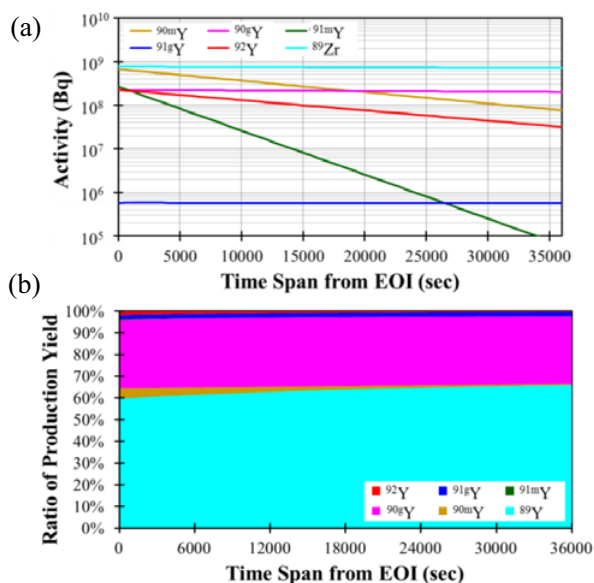


**Figure 7.** (a) Activity of  $^{92}\text{Y}$  and by-products as a function of time and (b) time variation of isotopic ratio of yttrium isotopes produced from  $^{\text{nat}}\text{Zr}$  target.

Figure 8(a) and (b) show the time variation of the activity of the  $^{92}\text{Y}$  and by-products, and the yields of carriers when 20 g of 100% enriched  $^{92}\text{Zr}$  is used.

The activity of  $^{92}\text{Y}$  at the EOI is 1.3 GBq, and is enough for SPECT studies. When using enriched  $^{92}\text{Zr}$ , the only problematic nuclides are  $^{91\text{m}}\text{Y}$  and  $^{91\text{g}}\text{Y}$ . Additional dose caused by the by-products are small and not critical. In addition, the isotopic purity is more than 90% for 5 hours and it is enough for labelling. However, as enriched  $^{92}\text{Zr}$  is very expensive, a high-efficiency target recycling technique needs to be developed in the future.

## 6. Conclusion

We proposed a new route to produce  $^{92}\text{Y}$  for bioscan prior to radiotherapy by means of  $^{90}\text{Y}$ -labelled ibiritumomab tiuxetan. Feasibility studies have been performed on the AVF cyclotron at CYRIC, Tohoku University, to determine the suitability of the  $C(d,n)$  accelerator-based neutrons for the  $^{92}\text{Zr}(n,p)^{92}\text{Y}$  reaction at 20 MeV of incident deuteron energy. We have found that  $^{92}\text{Y}$  of appropriate purity can be produced if an enriched  $^{92}\text{Zr}$  target is used. However, under these circumstances, a new chemical technique is required to recycle the very expensive target material at high yield.

In the present study, we have proposed the  $(d,n)$  neutron source using carbon target, because it has no toxicity, and low risk of target blistering effect. However,

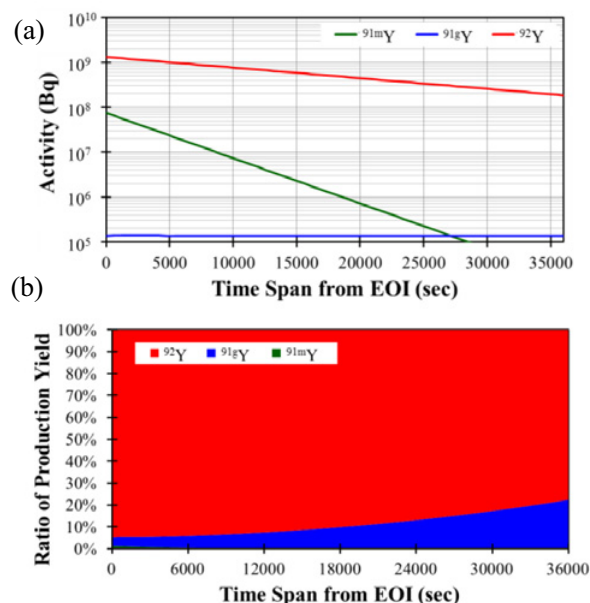


**Figure 8.** (a) Activities of  $^{92}\text{Y}$  and by-products as a function of time and (b) time variation of isotopic ratio of yttrium isotopes produced from 100% enriched  $^{92}\text{Zr}$  target.

in the future, beryllium or lithium target should also be investigated as stronger accelerator-based neutron source.

The authors would like to convey special thanks to all staffs at the Cyclotron Radioisotope Center for their fine efforts in providing high-quality beams.

## References

- [1] Biogen Idec Inc. Zevalin (ibritumomab tiuxetan) (Biogen Idec Inc., San Diego, CA, 2005)
- [2] T.E. Witzig, et al., *J. Clin. Oncol.* **20**, 3262 (2002)
- [3] F.F. Knapp, et al., *Eur. J. Nucl. Med.* **21**, 1151 (1994)
- [4] BLA 125019/194 supplement, dated January 20, 2011 (eCTD Sequence 0276)
- [5] H. Herzog, et al., *J. Nucl. Med.* **34**, 2222 (1993)
- [6] Y. Nagai, et al., *J. Phys. Soc. Jpn.* **82**, 064201 (2013)
- [7] K. Shibata, et al., *J. Nucl. Sci. Technol.* **48**, 1 (2011)
- [8] M.I. Majah et al., *J. Nucl. Sci. Eng.* **104**, 271 (1990)
- [9] P. Raics, et al., *Conf. on Nucl. Data for Sci. and Technol.*, 660 (1991)
- [10] V. Semkova, et al., *J. Nucl. Phys. A* **832**, 149 (2010)
- [11] S. Nakayama, et al., *Phys. Rev. C* **94**, 014618 (2016)
- [12] NEA, UMG 3.3, NEA-1665/03 (2004)
- [13] T. Sato, et al., *J. Nucl. Sci. Technol.* **50**, 913 (2013)
- [14] K.A. Weaver, et al., *Nucl. Sci. Eng.* **52**, 35 (1973)
- [15] O. Iwamoto, *J. Nucl. Sci. Technol.* **44**, 687 (2007)
- [16] O. Iwamoto, et al., *Nucl. Data Sheets* **131**, 259 (2016)